

ORIGINAL ARTICLE

Spatial distribution of ammonia-oxidizing bacteria and archaea across a 44-hectare farm related to ecosystem functioning

Ella Wessén¹, Mats Söderström², Maria Stenberg², David Bru^{3,4}, Maria Hellman¹, Allana Welsh¹, Frida Thomsen⁵, Leif Klemmedtson⁵, Laurent Philippot^{3,4} and Sara Hallin¹
¹Department of Microbiology, Swedish University of Agricultural Sciences, Uppsala, Sweden; ²Department of Soil and Environment, Swedish University of Agricultural Sciences, Skara, Sweden; ³INRA, UMR 1229, Dijon, France; ⁴Université de Bourgogne, UMR 1229, Dijon, France and ⁵Department of Plant and Environmental Sciences, University of Gothenburg, Göteborg, Sweden

Characterization of spatial patterns of functional microbial communities could facilitate the understanding of the relationships between the ecology of microbial communities, the biogeochemical processes they perform and the corresponding ecosystem functions. Because of the important role the ammonia-oxidizing bacteria (AOB) and archaea (AOA) have in nitrogen cycling and nitrate leaching, we explored the spatial distribution of their activity, abundance and community composition across a 44-ha large farm divided into an organic and an integrated farming system. The spatial patterns were mapped by geostatistical modeling and correlations to soil properties and ecosystem functioning in terms of nitrate leaching were determined. All measured community components for both AOB and AOA exhibited spatial patterns at the hectare scale. The patchy patterns of community structures did not reflect the farming systems, but the AOB community was weakly related to differences in soil pH and moisture, whereas the AOA community to differences in soil pH and clay content. Soil properties related differently to the size of the communities, with soil organic carbon and total nitrogen correlating positively to AOB abundance, while clay content and pH showed a negative correlation to AOA abundance. Contrasting spatial patterns were observed for the abundance distributions of the two groups indicating that the AOB and AOA may occupy different niches in agro-ecosystems. In addition, the two communities correlated differently to community and ecosystem functions. Our results suggest that the AOA, not the AOB, were contributing to nitrate leaching at the site by providing substrate for the nitrite oxidizers.

The ISME Journal (2011) 5, 1213–1225; doi:10.1038/ismej.2010.206; published online 13 January 2011

Subject Category: microbial ecology and functional diversity of natural habitats

Keywords: agricultural soil; ammonia oxidation; *amoA*; AOA; AOB; nitrate leaching

Introduction

Soil microorganisms are an integral part of the biogeochemical cycles and have key roles in ecosystem functioning. To increase our understanding of the mechanisms driving the distribution of microorganisms and the processes shaping these communities, characterization of their spatial patterns at various scales has become of great interest. Spatial analysis of microbial diversity have revealed a significant effect of distance on the taxa distribution of soil microorganisms ranging from a few centimeters to meters and even kilometer at the

landscape scale (Franklin and Mills, 2003; Ritz *et al.*, 2004; Dequiedt *et al.*, 2009; Philippot *et al.*, 2009a). However, Green *et al.* (2008) recently underlined the importance of focusing on trait-based rather than taxonomic biogeography in microbial ecology similar to what has been done for example in plant ecology (Enquist *et al.*, 2007; Savage *et al.*, 2007). This will aid in linking functional trait variation of microorganisms to ecosystem processes. Spatial analysis of abundance or diversity of functional microbial communities in soil have previously been investigated (Grundmann and Debouzie, 2000; Zhou *et al.*, 2008; Bru *et al.*, 2010), but seldom in relation to soil ecosystem functioning. A few attempts have been made in studies focusing on nitrogen cycling communities. For example, the distribution of the fraction of bacteria with the genetic capacity to reduce N₂O to N₂ was linked to areas with low potential N₂O emissions in a pasture (Philippot *et al.*, 2009b).

Correspondence: S Hallin, Department of Microbiology, Swedish University of Agricultural Sciences, Box 7025, Uppsala 750 07, Sweden.

E-mail: Sara.Hallin@mikrob.slu.se

Received 5 August 2010; revised 1 December 2010; accepted 1 December 2010; published online 13 January 2011

Enwall *et al.* (2010) further showed that a map of denitrification activity across an entire farm was reflected by maps displaying the community size and structure of a specific fraction of the denitrifiers at the site.

Since the fairly recent discovery that archaea, and not only bacteria, are capable of ammonia oxidation (Venter *et al.*, 2004; Könneke *et al.*, 2005; Treusch *et al.*, 2005), there has been a vivid interest in identifying the specific drivers of the ammonia-oxidizing bacteria (AOB) and archaea (AOA), and answering questions regarding their respective contribution to ammonia oxidation and ecosystem functions (Leininger *et al.*, 2006; He *et al.*, 2007; Chen *et al.*, 2008; Shen *et al.*, 2008; Tourna *et al.*, 2008; Jia and Conrad, 2009; Mertens *et al.*, 2009; Schauss *et al.*, 2009). Ammonia oxidation is the first and rate limiting step in the nitrification process, the oxidation of ammonium (NH_4^+) via nitrite (NO_2^-) to nitrate (NO_3^-) and is of great environmental and agronomical interest because of the conversion of the relatively immobile nitrogen form NH_4^+ to the highly mobile form NO_3^- leading to nitrogen losses from soil by run-off and leaching. Moreover, nitrification is also one of the terrestrial sources of N_2O , which is a potent greenhouse gas with a global warming potential of c.a. 300 times that of the CO_2 (Conrad, 1996; IPCC Core Writing Team, 2007). Because of these concerns and the role of ammonia oxidizers in nitrogen cycling in general, understanding the spatial distribution of the AOA and AOB in relation to ecosystem functioning and soil properties is important, especially in agro-ecosystems.

In this study, we present a comprehensive analysis of the spatial distribution and putative soil factor determinants of both the size and structure of the bacterial and archaeal ammonia-oxidizing communities across a 44-ha farm divided into an integrated and an organic farming system. A geo-statistical approach was used to map and predict the spatial distribution of the AOA and AOB communities. We further examined how these spatial patterns and the soil properties were related to the distribution of the community function assessed as substrate-induced ammonia-oxidation (SIAO) rates and *in situ* ecosystem functioning in terms of nitrate leaching.

Materials and methods

Field site, soil sampling and nitrate leaching

Logården research farm is located in Sweden ($58^\circ 20' \text{N}$, $12^\circ 38' \text{E}$, altitude 50 m) and since 1991 the 44-ha farm has consisted of one integrated (26 ha) and one organic farming system (18 ha), each with an individual 7-year crop rotation that includes green manure leys and faba beans. The integrated farming system is managed by optimizing inputs, while the organic farming system is managed according to the Swedish criteria for organic farming

and is entirely dependent on leguminous plants with symbiotic N-fixation for nitrogen supply. The soil type varies from a silty clay loam to silty clay soil of postglacial origin with an average clay content of about 40% and organic matter content of 2–3% (Supplementary Table S1).

Each farming system has fixed sampling locations, 51 in total for both systems, which are used in a monitoring program (Figure 1). A total of 12 soil cores (20 mm diameter) were sampled at 10 cm depth at each of the 51 fixed locations in April 2007 and pooled into one sample per location. After sieving (4 mm) the soil physical and chemical parameters were determined and then the soil was stored at -20°C according to recommendations by Stenberg *et al.* (1998) before analysis of SIAO rates and DNA extraction.

Each farming system is divided into seven fields and all 14 fields are equipped with separate drainage systems and wells, except fields C1 and C3 that have separate drainage in the west and east parts of the fields resulting in two wells in each of

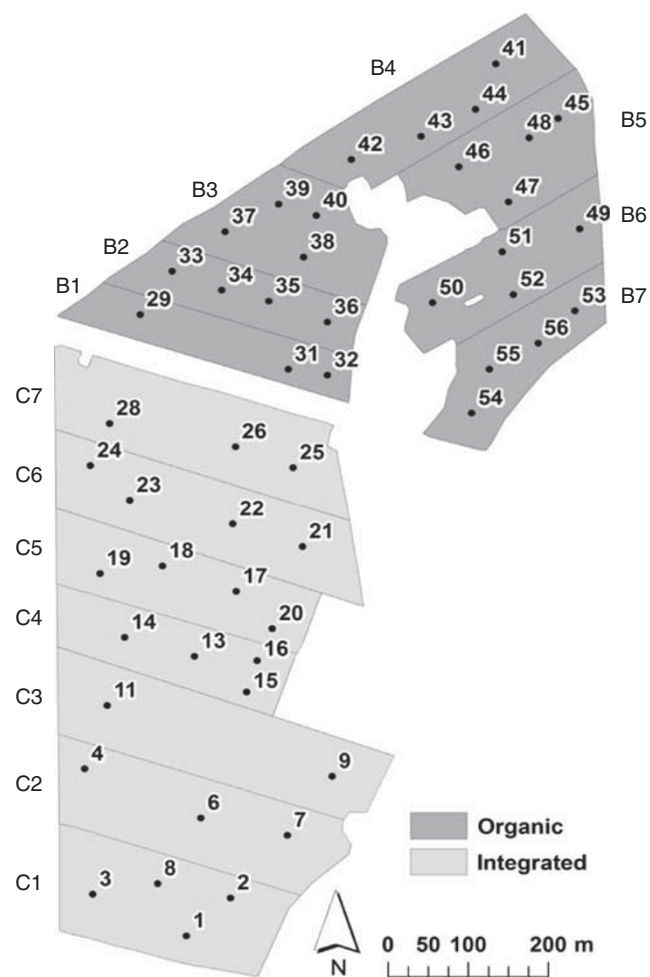


Figure 1 Map of Logården experimental farm (44 ha) divided into an integrated crop production system (26 ha; samples 1–28; fields C1–C7) and an organic crop production system (18 ha; samples 29–56; fields B1–B7). Sample sites, field borders and numbers are indicated.

these two fields. Thus, leaching was measured in 16 wells and the amount of nitrogen in the drainage water was recorded every second week from July 2004 to June 2008. Discharge was measured continuously in each well through a V-over-fall at the side of a half circular stainless steel container with open top (Supplementary Figure S1). The height in the V was calibrated to a plastic cylindrical body hanging in a loading cell connected to a data logger. Discharge was calculated on a daily basis. Automatic sampling of water was carried out flow-proportional; that is, for every 0.15-mm discharge a 10 ml sample was poured into a 10 l flask. The flask was emptied manually every second week and a sub-sample was taken for analyses after careful mixing of the 10 l sample. Total N concentrations was determined by oxidizing inorganic and organic N constituents by $K_2(SO_4)_2 + NaOH$ to NO_3^- , which was analyzed by flow-injection analysis (Tecator AB, Höganäs, Sweden) according to the colorimetric Cd-reduction method (APHA, 1985). Nitrate in the water was analyzed colorimetrically according to the method SS 028133-2 SS-EN ISO 13395-1 at an accredited laboratory.

Soil parameters

Total nitrogen (Tot-N) was measured as Kjeldahl-N (ISO 13878) and NO_3^- and NH_4^+ were extracted with 2 M KCl and determined with flow injector analysis. Total carbon was determined by dry combustion (ISO 10694). Dissolved organic carbon and dissolved organic nitrogen were extracted from 5 g of soil by adding 500 ml distilled water, shaking for 2 h, centrifugation at 2500 r.p.m. for 20 min and filtration (0.45 μ m). The dissolved organic carbon was determined with a TOC Analyzer (Teledyne Tekmar, Mason, OH, USA) and dissolved organic nitrogen was calculated as the difference between Kjeldahl-N and NH_4^+ -N. The pH was defined in 0.01 M $CaCl_2$ (ISO 10390). Water content and dry weight (dw) was determined in all soil samples by drying for 72 h at 105 °C. The clay content in the top-soil was previously estimated using near-infra-red determinations calibrated from the particle size analyzed samples (Wetterlind *et al.*, 2005).

Substrate-induced ammonia oxidation (SIAO) rate

The SIAO rate was measured as accumulated nitrite according to a short incubation, chlorate inhibition technique (Belser and Mays, 1980; Torstensson, 1993) (ISO 15685). In brief, 100 ml of 1 mM potassium phosphate buffer (pH 7.2) containing 0.4 mM (di)-ammonium sulfate and 15 mM sodium chlorate was added to 25 g soil that was incubated on a rotary shaker at 25 °C for 5 h. Aliquots of 2 ml were taken once every hour and the nitrite concentration was determined by flow injection analysis (FIA, Tecator AB). The SIAO rates were calculated by linear

regression of the accumulated NO_2^- -N per g dw soil over time.

DNA extraction

DNA was extracted in duplicate from a total of 1 g soil from each sample using the FastDNA SPIN for Soil Kit (MP Biomedicals, Santa Ana, CA, USA) according to the manufacturer's instructions. The two resulting DNA extractions per sample were pooled before further analysis. DNA was quantified by spectrophotometry at 260 nm using a BioPhotometer (Eppendorf, Hamburg, Germany).

Real-time PCR quantification of AOB and AOA *amoA* genes

Real-time quantitative PCR of the *amoA* genes was performed to estimate the abundance of the ammonia-oxidizing bacterial and archaeal communities. The primers *amoA*-1F (5'-GGGGTTTCTACTGGTGGT-3') and *amoA*-2R (5'-CCCCTCKGSAAAGCCTTC TTC-3') were used for bacteria generating a 491 bp fragment (Rotthauwe *et al.*, 1997); and *CrenamoA23f* (5'-ATGGTCTGGCTWAGACG-3') and *CrenamoA616r* (5'-GCCATCCATCTGTATGTCCA-3') were used for archaea generating a 628 bp fragment (Tourna *et al.*, 2008). Quantification was based on the fluorescence intensity of the SYBR Green dye in a total volume of 20 μ l using Absolute QPCR SYBR Green Rox (ABgene, Courtaboeuf, France), 1 μ M of each primer, 10 ng of soil DNA and 0.5 μ g T4Gp32 (QBiogene, Illkirch, France), and reactions were performed in two independent PCR reactions in an ABI7900HT thermal cycler (Applied Biosystems, Carlsbad, CA, USA). All reactions were finished with a melting curve starting at 80 °C with an increase of 0.5 °C up to 95 °C. The PCR efficiency ranged between 83 and 100%. Standard curves were obtained using serial dilutions of linearized plasmids (pGEM-T) containing cloned *amoA* genes. Controls without templates resulted in values lower than the detection limit or negligible values. Inhibitory effects on PCR performance was tested for all samples by mixing a known amount of the pGEM-T plasmid with the soil DNA extracts or water before running a qPCR with the plasmid specific T7 and SP6 primers. The measured cycle threshold (C_t) values obtained for the different DNA extracts and the controls with water were not significantly different indicating that no inhibition occurred.

Terminal-restriction fragment length polymorphism (T-RFLP) analysis of AOB and AOA *amoA* genes

PCR amplification of the *amoA* genes for the AOB and the AOA were done in duplicate for each sample using the same primers as for the quantification, except that the forward primer was labeled at the 5' end with hexachlorofluorescein (HEX). Each reaction was performed in a total volume of 50 μ l containing 40 or 5 ng of soil DNA for AOB and AOA,

respectively, 5 μ l 10 \times PCR buffer, 0.4 μ M of each primer, 200 μ M (each) deoxyribonucleoside triphosphate, 2.5 U of Taq DNA polymerase and BSA was added to reach final concentrations of 800 ng μ l⁻¹. The PCR was performed in a GeneAmp PCR System 9700 machine (Applied Biosystems, Singapore, Singapore) according to Rotthauwe *et al.* (1997) for the AOB, with the modification of only running 30 cycles, and according to Sahan and Muyzer (2008) for the AOA.

The duplicated PCR reactions for each DNA extract were pooled and divided in three portions after which the AOB amplicons were digested with 10 U of the enzymes *Acil*, *Sau96I*, and *HpyCH4IV* and the AOA amplicons were digested with 10 U of *Acil*, *AluI* and *RsaI* during 2 h according to the instructions provided by the manufacturer (New England Biolabs, Ipswich, MA, USA). The enzymes were selected based on results from pre-experiments with several different enzymes on the samples (data not shown). The resulting terminal-restriction fragment (TRF) patterns were evaluated using the software Peak Scanner v.1.0 (Applied Biosystems) and fragments smaller than 50 bp and contributing with < 1% of the total signal were excluded from the subsequent analysis.

Cloning, sequencing and phylogenetic analysis of AOB and AOA amoA genes

To confirm the phylogenetic affiliation of the AOB and AOA community members and identify specific TRFs in terminal-restriction fragment length polymorphism (T-RFLP) electropherograms, bacterial and archaeal *amoA* genes were cloned and sequenced using DNA pooled from all sampling locations. The PCR reactions for each gene were conducted in duplicate as described for the T-RFLP analysis of AOB and AOA *amoA* genes, but without HEX-labeled primers. The PCR products were gel purified using QIAquick Gel Extraction Kit (Qiagen, Hilden, Germany) and cloned using the TOPO TA Cloning Kit for Sequencing (Invitrogen, Carlsbad, CA, USA). Two clone libraries were constructed for the AOB and AOA, respectively, and 96 clones of each group were sequenced by Macrogen Inc. (Seoul, Korea) with an ABI3730XL automatic DNA sequencer.

Nucleotide sequences were aligned using Geneious v5.0.4 (Biomatter Ltd, Auckland, New Zealand) with the ClustalW alignment algorithm (Thompson *et al.*, 1994). The final data sets included 90 and 92 AOB and AOA sequences with 453 and 603 bp, respectively. Sequences from pure cultures and uncultured environmental sequences identified by a blastn search (Altschul *et al.*, 1990) were incorporated into the alignment. Maximum likelihood phylogenetic analyses were completed using the RAxML-VI-HPC BlackBox program v7.2.6 (Stamatakis, 2006; Stamatakis *et al.*, 2008) on the CIPRES computer cluster from the online servers at the San Diego Supercomputing Center

(<http://www.phylo.org>). The *amoA* sequences were *in silico* digested with the same enzymes that were used in the T-RFLP analysis and the resulting TRFs were compared with those generated in the *in vitro* analysis using Geneious. TRFs with differences ≤ 2 bp were considered as the same genotype.

Statistical analysis

Pairwise correlations between soil parameters, SIAO rates, nitrate leaching and abundance of AOB and AOA communities were done using Pearson's correlation coefficient or Spearman's rho, depending on whether data were normally distributed or not, (Pearson, 1896; Spearman, 1904) using XLSTAT Version 2009.5.01 (Addinsoft, New York, NY, USA). Relationships between the differences in the composition of the AOB and AOA communities and differences in soil parameters, SIAO rates and nitrate leaching were determined using the Mantel test (Mantel, 1967). The Bray–Curtis distance measure was used for correlating distances matrices based on the relative abundance of TRFs with Monte Carlo simulations (999 randomizations). The structure of AOB and AOA communities based on the relative abundance of TRFs were also analyzed by non-metric multidimensional scaling (NMS), and the Bray–Curtis distance measure was used to generate dissimilarity matrices. Soil parameters, SIAO rates and data on nitrate leaching were incorporated into the analysis through the use of bi-plot ordinations where all variables were combined into a secondary matrix and plotted as vector fits against community composition ordinations. The data in the second matrix were relativized by dividing values within each variable by column totals. The NMS was run using a random starting configuration, a maximum of 250 iterations and an instability criterion of 0.00001 and performed on 200 runs with the real data and 200 runs with randomized data to test for the null hypothesis. The ordination was rotated to maximize variance explained by the different parameters included in the analysis. For a two-dimensional solution with the lowest possible stress value, a final run using the best starting configuration from the first run was performed. Both the Mantel tests and the NMS were done using PC-ORD version 5.10 (MjM Software, Gleneden Beach, OR, USA).

Geostatistical modeling and mapping

Moran's *I* index (Moran, 1950) was used to assess the presence of global spatial autocorrelation for the different variables. This was done for all data ($n = 51$), as well as separately for the observations within the two different farming systems (Supplementary Table S2). Variables for the community structure were obtained by using the sample scores for the first axis in the NMS-analyses of the T-RFLP profiles for both the bacterial and archaeal *amoA*

genes. The *Z*-score and *P*-value were estimated to evaluate the significance of the index. The variables were modeled geostatistically (Isaaks and Srivastava, 1989) when index values were significant (Z -score > 1.96 ; $P < 0.05$) using the software GS+ version 9 (Gamma Design Software, Plainwell, MI, USA) for the variogram analysis. The variograms were evaluated by cross-validation, that is, one sampling point was removed at a time and the variogram model was tested on the sample omitted. The root mean square error of prediction and the ratio of performance of deviation (RPD, that is, the s.d. divided by the root mean square error of prediction) were calculated for each parameter (Supplementary Table S3). Ordinary kriging, which is a technique for spatial estimation through which the selection of weights is made such that the estimation variance is minimized and the geographical information system ArcGIS 9.3 (ESRI Inc., Redlands, CA, USA) with the extension Geo-statistical Analyst were used for interpolation and mapping.

Nucleotide sequence accession numbers

The *amoA* sequences for the AOB and AOA have been deposited in GenBank under accession number HQ638885 through HQ638974 and HQ638793 through HQ638884, respectively.

Results

Distribution of the AOB and AOA community size in relation to soil parameters

The number of bacterial *amoA* genes was in the range of 5.6×10^6 – 1.7×10^7 gene copies per g dw soil, whereas the crenarchaeal *amoA* genes varied between 8.8×10^6 – 6.0×10^7 gene copies per g dw soil (Supplementary Table S1). This corresponded to 3.9×10^2 – 1.0×10^3 and 6.3×10^2 – 4.1×10^3 gene

copies per ng DNA for the AOB and AOA, respectively. The AOB abundance was significantly higher in the integrated farming system compared with the organic farming system ($P < 0.05$), but no significant difference was found between farming systems for the AOA abundance. The sizes of both the AOB and AOA communities expressed per g dw soil exhibited spatial dependence with autocorrelation ranging between 130 and 140 m across the 44-ha farm area (Figures 2a and b). The patterns were patchy for both groups of ammonia oxidizers, although the AOA were more evenly distributed in the organic farming system. The spatial patterns of the AOA community size expressed per ng DNA (Supplementary Figure S2a) was nearly identical to patterns observed for the AOA expressed per g dw soil. However, for the AOB this similarity was only found in the integrated farming system because of the lack of spatial autocorrelation for the AOB community size expressed per ng DNA in the organic system (Supplementary Figure S2b and Supplementary Tables S2 and S3). The low RDP- and *Z*-score values for all abundance data in the organic farming system (Supplementary Table S2) give the generated maps an uncertainty and thus, the spatial patterns in the integrated system were more robust.

In the integrated farming system the highest abundances of AOB were predicted in the southern parts of the farm, whereas the lowest were observed in the central areas. Interestingly, the spatial patterns of the size of the AOA community displayed the opposite pattern with lowest abundance in the southern fields and increased community size in the central area. This was reflected in the spatial pattern of the AOA:AOB ratio, which largely followed that detected for the AOA abundance (Figure 2c; Supplementary Tables S2 and S3). The AOA:AOB abundance ratio varied from 0.7 to 7.8

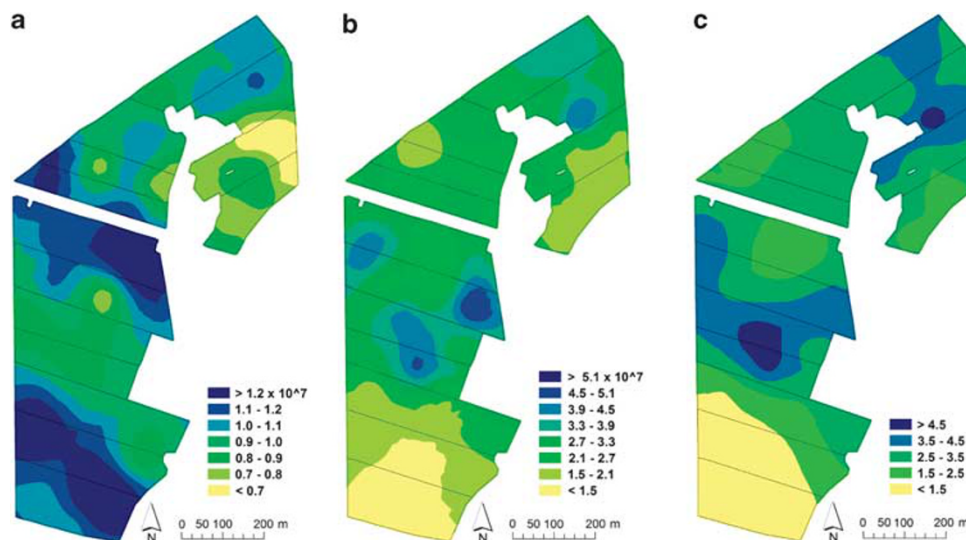


Figure 2 Kriged maps of the distribution of the AOB and AOA community sizes. (a) AOB *amoA* gene copy numbers (per g dw soil), (b) AOA *amoA* gene copy numbers (per g dw soil) and (c) ratio between AOA and AOB *amoA* gene copy numbers.

(Supplementary Table S1) and no significant difference between the two farming systems was observed. Correlations between the bacterial and archaeal *amoA* gene copy numbers and the nine chemical and physical soil parameters measured at each sampling site revealed that different soil parameters were related to the size of the AOB and AOA communities indicating a niche differentiation between these two groups (Table 1). Soil total carbon and Tot-N correlated positively to the AOB abundance ($r=0.39$ and $r=0.28$; $P\leq 0.01$ and $P<0.05$, respectively), whereas predicted clay content and pH correlated negatively to the AOA abundance ($r=-0.56$ and $r=-0.33$; $P\leq 0.001$ and $P<0.05$, respectively).

Distribution of the AOB and AOA community structure in relation to soil parameters

The T-RFLP profiles of the amplified *amoA* genes from the AOB and AOA communities generated by each enzyme consisted of two to four dominant and several minor peaks. The average numbers of peaks in the stacked profiles of the three enzymes were 11 for the AOB and 12 for the AOA. The NMS ordinations of the T-RFLP profiles of bacterial and archaeal *amoA* genes revealed that the community structure of the AOB and AOA differed between sampling locations (Figure 3). The analyses were supported by low final stress values (9.2 and 6.6), the Monte Carlo test ($P<0.001$; 999 runs) and the strong correlation between distances in the

Table 1 Pearson's correlations (r) between SIAO, community size (qAOB, qAOA and AOA/AOB) and soil properties (Clay, pH, dw, $\text{NH}_4\text{-N}$, $\text{NO}_3\text{-N}$, Tot-C, Tot-N, C/N, DON and DOC) measured at each individual sampling point ($n=51$)

	SIAO	qAOB	qAOA	AOA/AOB	Clay ^a	pH ^a	Dw	$\text{NH}_4\text{-N}$	$\text{NO}_3\text{-N}$	Tot-C	Tot-N	C/N	DON	DOC
SIAO	1	NS	NS	NS	NS	**	NS	NS	NS	NS	NS	NS	NS	*
qAOB	0.04	1	NS	***	NS	NS	NS	NS	NS	**	*	NS	NS	NS
qAOA	-0.14	-0.03	1	***	***	*	NS	NS	NS	NS	NS	NS	NS	NS
AOA/AOB	-0.20	-0.52	0.84	1	***	NS	NS	NS	NS	NS	NS	NS	NS	NS
Clay	0.27	-0.02	-0.56	-0.47	1	NS	*	NS	NS	NS	NS	NS	NS	NS
pH	0.42	-0.14	-0.33	-0.24	0.18	1	NS	NS	NS	*	NS	NS	NS	*
dw	0.00	-0.04	0.13	0.07	-0.26	-0.15	1	*	NS	***	**	NS	*	*
$\text{NH}_4\text{-N}$	-0.16	0.19	0.07	0.01	-0.09	-0.15	-0.35	1	NS	**	**	NS	***	NS
$\text{NO}_3\text{-N}$	0.14	0.21	-0.09	-0.18	0.02	0.08	-0.20	-0.13	1	**	NS	NS	NS	NS
Tot-C	0.00	0.39	0.10	-0.05	0.01	-0.33	-0.47	0.40	0.36	1	***	***	**	NS
Tot-N	-0.05	0.28	0.15	-0.04	0.07	-0.22	-0.41	0.37	0.21	0.60	1	NS	**	NS
C/N	0.05	0.20	0.01	-0.002	-0.10	-0.16	-0.17	0.12	0.23	0.65	-0.23	1	NS	*
DON	-0.17	0.13	0.05	0.05	-0.14	-0.07	-0.31	0.70	0.20	0.36	0.39	0.05	1	NS
DOC	0.30	-0.14	0.03	0.11	-0.02	0.30	-0.34	0.05	0.08	0.14	-0.13	0.30	-0.08	1

Abbreviations: AOA, ammonia-oxidizing archaea; AOB, ammonia-oxidizing bacteria; Clay, predicted clay content; DOC, dissolved organic carbon; DON, dissolved organic nitrogen; dw, dry weight; NS, not significant; SIAO, substrate-induced ammonia oxidation; Tot-C, total organic carbon; Tot-N, total nitrogen.

Values in bold are statistically significant. *** $P\leq 0.001$; ** $P\leq 0.01$; * $P\leq 0.05$.

^aSpearman's correlations were used as data were not normally distributed.

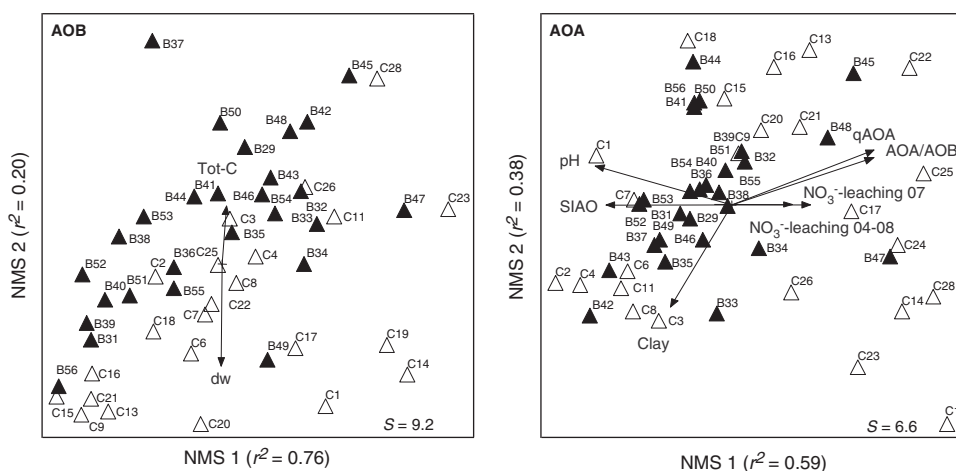


Figure 3 Non-metric multidimensional scaling analysis of the AOB and AOA community structure based on T-RFLP analysis of *amoA* genes. Sampling locations from the organic (▲) and integrated (△) farming system are indicated by numbers. Soil properties (Supplementary Table S1), abundances of *amoA* for AOB and AOA (qAOB, qAOA), qAOA/qAOB ratios, SIAO rates and nitrate leaching between June 2004 and July 2008, as well as only in 2007 ($\text{NO}_3\text{-leaching}$ 04-08 and $\text{NO}_3\text{-leaching}$ 07) were incorporated in the analysis. Only those that were significant are shown. The arrow length is proportional to the strength of correlation and the orientation indicates the direction in which they have maximum correlation with the ordination configuration. The proportion of variance is represented by each axis, based on the r^2 between distance in the ordination space and the original space is indicated in addition to stress values (S).

two-dimensional ordination space and the original space ($r^2=0.96$ and $r^2=0.97$ for AOB and AOA, respectively). The dominant peaks in the T-RFLP profiles of the AOB and AOA communities and their distribution across sampling locations are shown in Supplementary Figures S3 and S4, respectively.

The sample scores on axes 1 in the ordinations for the AOB ($r^2=0.76$) and AOA ($r^2=0.59$) communities were used as variables in the geostatistical modeling of the composition of the two communities, which are displayed in the kriged maps (Figure 4; Supplementary Tables S2 and S3). The AOB community composition differed in the integrated farming system between east and west and had a more patchy distribution in the organic system. These differences were not explained by the soil properties, but there was a tendency for a separation between the community structure in the organic and integrated farming system that correlated to the soils decreasing carbon content (total carbon) and increasing dw in the integrated system (Figure 3). When considering the differences in AOB community composition across all locations, the AOB correlated only weakly to differences in several soil properties with pH and soil dw having the strongest correlations ($r^{\text{Mantel}}=0.13$; $P\leq 0.01$ and $r^{\text{Mantel}}=0.14$; $P\leq 0.01$; Table 2). The AOA community composition was rather heterogeneous in the integrated system, but in contrast to the AOB it

differed in a south-north direction. The variation in AOA community composition was small in the organic farming system. The distribution of AOA genotypes also correlated weakly with some differences in soil properties, mostly clay content and pH ($r^{\text{Mantel}}=0.17$; $P<0.05$ and $r^{\text{Mantel}}=0.18$; $P\leq 0.01$; respectively, Table 2).

Phylogenies of AOB and AOA amoA genes and identity of TRFs

The distribution of the relative abundances of several dominant TRFs across the sampling locations differed along axes 1 (Supplementary Figures S3 and S4), indicating that different bacterial and archaeal *amoA* genotypes were associated with the observed patterns. These differences prompted us to identify the dominant TRFs explaining the distributions. The phylogenetic analyses revealed that sequences obtained using the AOB primers were similar to environmental *amoA* clones related to *Nitrosospira* spp. For the crenarchaeal *amoA* sequences, two clones were in a well-supported group with *Nitrosopumilis maritimus*, while the others were grouped with *Nitrososphaera gargensis* (Supplementary Figures S5 and S6). Except for one of the archaeal *amoA* sequences in the *Nitrosopumilis maritimus* lineage, each cloned sequence contained terminal restriction sites that could be

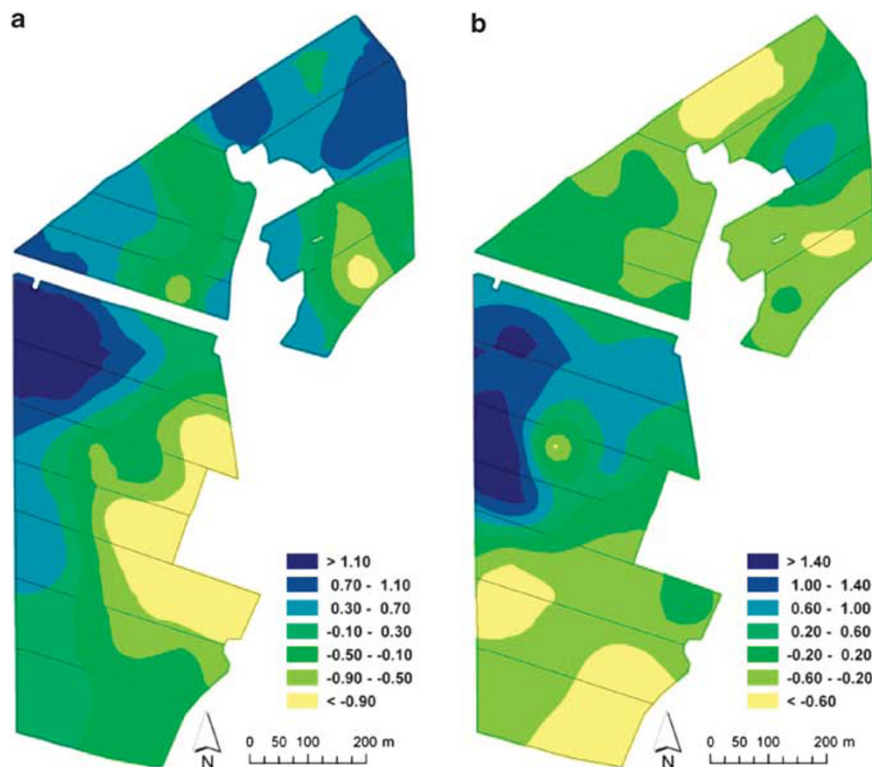


Figure 4 Kriged maps of the AOB and AOA community structure based on the sample scores on axis 1 in the NMS analysis of the T-RFLP profiles of *amoA* genes (Figure 3), thus, reflecting the community composition reduced to one dimension. (a) The AOB community structure. (b) The AOA community structure. The numbers in the panels refer to the scores on axis 1 in the NMS.

linked to a corresponding TRF in the community profile. Eight dominant AOB and AOA TRFs were identified to influence the analyses of the community composition of the two groups (Supplementary Figures S3 and S4). For example, in the heterogeneous integrated farming system, the AOB community composition in the western parts was related to the increased abundances of TRFs *Acil*-117 and *Sau96I*-168, while the east parts were dominated by *Acil*-129 and *Sau96I*-179 (Supplementary Figure S3). Samples at these eastern locations also had a low abundance of *HpyCH4IV*-417 TRFs. Sequences with TRFs *Acil*-117 and *Sau96I*-168 were found in a monophyletic group including the pure culture *Nitrospira* sp. CT2F. However, TRFs *Acil*-129, *Sau96I*-179, but also *Sau96I*-168 were associated with sequences across the tree (Supplementary Figure S5). For the AOA communities we could associate an increased abundance of TRFs *Acil*-203, *AluI*-166 and *RsaI*-296 with the upper west parts of the integrated farming system while *Acil*-380 and *AluI*-205 increased in the southern parts of this farming system (Supplementary Figure S4). Sequences containing the upper-west associated TRFs were found in a clade containing only soil-derived clones, except *AluI*-166 that was also associated to the *Nitrosopumilis maritimus* lineage. By contrast, sequences containing the southern-associated TRFs grouped with clones from varying environments, for example, soil, sediment and river water.

Community and ecosystem functions: ammonia oxidation and nitrate leaching

The SIAO rates varied between 1.0. and 7.2 ng NO_2^- -N per g dw soil per min (Supplementary Table S1). The activity exhibited spatial autocorrelations with rather similar rates distributed over the farm, except for the high rates observed in the southern parts of the integrated farming system (Figure 5; Supplementary Tables S2 and S3). Even though the ammonia-oxidation rates were relatively similar between farming systems, there was a significant difference between the systems ($P < 0.0001$) with a higher average rate in the integrated system, which was mainly explained by the higher activity found in the southern parts of farm.

The average amount of nitrate that had leached from the each field during the time period July 2004 to June 2008 ranged from 8.5 to 22.4 kg NO_3^- -N per ha per year and the average amount of Tot-N that had leached ranged from 11.5 to 28.5 kg NO_3^- -N per ha per year (Supplementary Table S1). This time period, flanking the sampling time, was used for data presentation to observe long-term trends by minimizing year-to-year variation within each field, which strongly depends on crop, fertilization and precipitation. During the year 2007 the amount of nitrate that had leached from the each field ranged from 2.5 to 22.5 kg NO_3^- -N per ha per year and the amount of leached Tot-N ranged from 6.5 to 26.9 kg

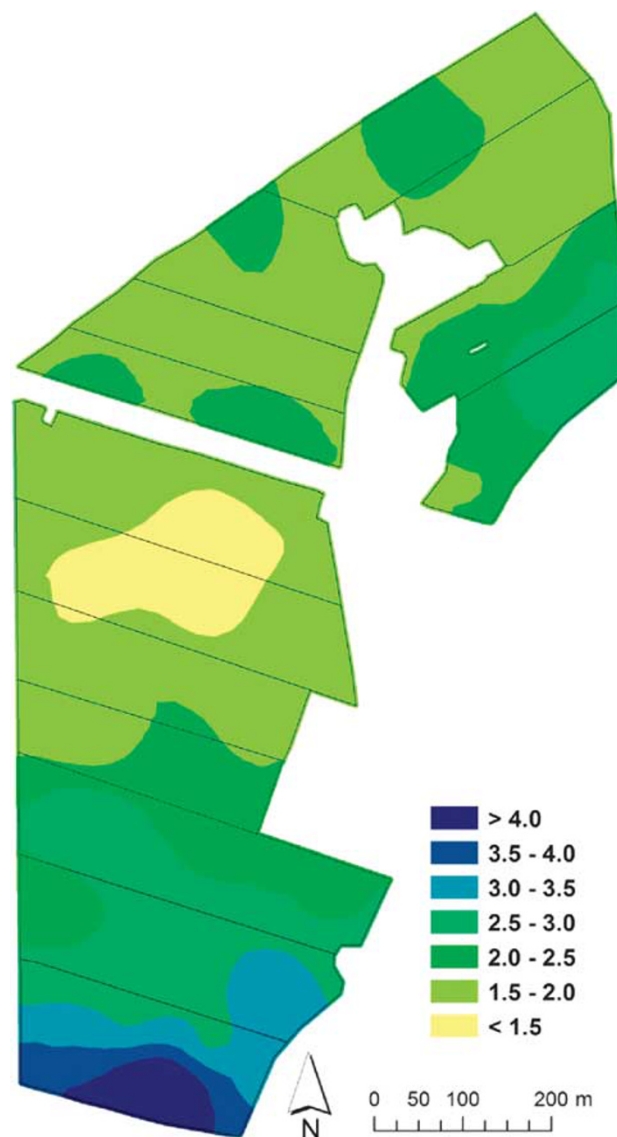


Figure 5 Kriged map of the distribution of the SIAO rate (ng NO_2^- -N per g dw soil per min).

NO_3^- -N per ha per year, thus being similar to the overall period that was observed (Supplementary Table S1). The average nitrate leaching varied between fields and in contrast to the ammonia-oxidation rates, less was being leached in the southern parts of the integrated farming system (Figure 6). The major fraction of the Tot-N in the drainage water was nitrate in both farming systems (Supplementary Table S1). This suggests that nitrification was occurring at the site, as the organic system was not fertilized with nitrate.

Possible correlations between ecosystem functioning, and abundance, activity and composition of the ammonia-oxidizing communities were explored to search for possible drivers underlying nitrate leaching (Tables 2 and 3). The SIAO rate was not related to differences in community composition of the

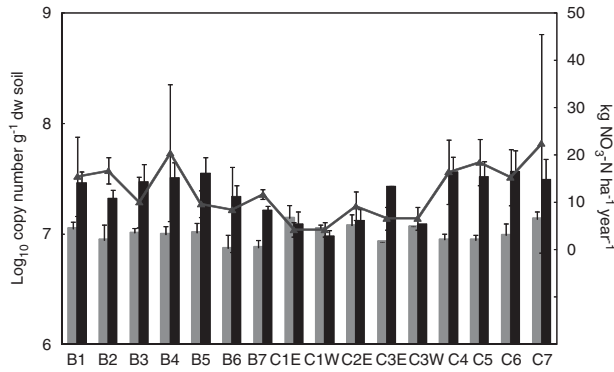


Figure 6 Nitrate leaching (NO_3^- -N kg per ha per year) during the time period June 2004–July 2008 (\blacktriangle) and the size of the AOB (gray bars) and AOA (black bars) community per field (mean \pm s.d.), except for fields C1 and C3, which have separate drainage systems in the east and west parts of the fields denoted as E and W, respectively below the bars.

bacterial or archaeal ammonia oxidizers (Table 2), but negatively related to the field averaged abundance of AOA ($r = -0.75$; $P \leq 0.001$; Table 3). The average nitrate leaching based on values from the entire period or only the values from 2007 correlated negatively to the ammonia-oxidation rates ($r = -0.63$ and $r = 0.57$; $P \leq 0.01$ and $P < 0.01$; Table 3). Interestingly, there was a positive correlation between nitrate leaching and the AOA abundance ($r = 0.67$; $P \leq 0.01$; Figure 6) and AOA/AOB abundance ratio ($r = 0.54$; $P < 0.05$) and an even stronger correlation was found when data on nitrate leaching from only year 2007, corresponding to the year of soil sampling, were used ($r = 0.79$; $P < 0.001$ and $r = 0.65$; $P < 0.01$, respectively; Table 3). Moreover the differences in community composition of AOA, but not those of the AOB, were significantly correlated with differences in the average nitrate leaching during the entire period ($r^{\text{Mantel}} = 0.18$; $P \leq 0.01$; Table 2), which is supported by the vector fit in the NMS ordination (Figure 3).

Discussion

The size and structure of the AOB and AOA communities at the Logården site were not randomly distributed but instead exhibited spatial patterns, which could be mapped using geostatistical modeling. These results agree with previous work showing that AOB and AOA communities exhibit biogeographical patterns across terrestrial ecosystems at larger scales (Fierer *et al.*, 2009; Bru *et al.*, 2010). Quantification of the size of the AOA and AOB communities at the Logården farm was, for most locations, consistent with previous studies showing a dominance of the AOA over the AOB (Leininger *et al.*, 2006; He *et al.*, 2007; Nicol *et al.*, 2008; Shen *et al.*, 2008). Interestingly, using the data from Enwall *et al.* (2010) from the same sampling

Table 2 The standardized Mantel statistics (r) of correlations between the dissimilarity matrices of community structure of AOB and AOA, ecosystem functions (NO_3^- -leaching between June 2004 and July 2008, as well as only in 2007 calculated as average values per drained field ($n = 16$)) and SIAO, community size (qAOB, qAOA and AOA/AOB) and soil properties (Clay, pH, dw, NH_4^+ -N, NO_3^- -N, Tot-C, Tot-N, C/N, DON and DOC), which were measured at each individual sampling point ($n = 51$)

	AOA structure	AOB structure	NO_3^- -leaching 04–08	NO_3^- -leaching 07	SIAO	qAOB	qAOA	AOA/AOB	Clay	pH	dw	NH_4^+ -N	NO_3^- -N	Tot-C	Tot-N	C/N	DON	DOC
AOB structure	0.33***	—	NS	NS	NS	NS	NS	NS	NS	0.13**	0.14**	0.07*	0.09**	0.11**	0.07*	NS	NS	NS
AOA structure	—	0.33***	0.19**	0.08*	NS	NS	0.23***	0.30***	0.17*	0.18**	NS	0.07*	0.11**	0.11**	0.10**	NS	NS	NS

Abbreviations: AOA, ammonia-oxidizing archaea; AOB, ammonia-oxidizing bacteria; Clay, predicted clay content; DOC, dissolved organic carbon; DON, dissolved organic nitrogen; dw, dry weight; NS, not significant; SIAO, substrate-induced ammonia oxidation; Tot-C, total organic carbon; Tot-N, total nitrogen. Values in bold are statistically significant. *** $P \leq 0.001$; ** $P \leq 0.01$; * $P \leq 0.05$.

Table 3 Pearson's correlations (*r*) between ecosystem functions (NO₃-leaching between June 2004 and July 2008, as well as only in 2007), SIAO, community size (qAOB, qAOA and AOA/AOB) and soil properties (Clay, pH, dw, NH₄-N, NO₃-N, Tot-C, Tot-N, C/N, DON and DOC) calculated as average values per drained field with 2–4 sampling points per field

	NO ₃ -leaching 04–08	NO ₃ -leaching 07	SIAO	qAOB	qAOA	AOA/AOB	Clay	pH ^a	dw	NH ₄ -N	NO ₃ -N	Tot-C	Tot-N	C/N	DON	DOC
NO ₃ -leaching 04–08	1															
NO ₃ -leaching 07	0.74	1														
SIAO	-0.63	-0.57	1													
qAOB	-0.09	-0.09	0.21	1												
qAOA	0.67	0.79	-0.75	-0.30	1											
AOA/AOB	0.54	0.65	-0.72	-0.60	0.92	1										
Clay	-0.45	-0.62	0.55	0.24	-0.75	-0.70	1									
pH	-0.44	-0.41	0.57	-0.04	-0.47	-0.30	0.28	1								
dw	0.02	0.12	0.04	-0.18	0.07	0.13	-0.41	-0.12	1							
NH ₄ -N	-0.02	0.25	-0.06	0.25	0.26	0.09	-0.08	0.11	-0.30	1						
NO ₃ -N	0.43	0.04	-0.02	0.37	-0.17	-0.34	0.00	0.08	-0.26	-0.16	1					
Tot-C	0.25	0.25	0.01	0.54	0.08	-0.20	0.060	-0.03	-0.46	0.45	0.52	1				
Tot-N	0.22	0.18	-0.21	0.60	0.09	-0.19	0.20	-0.23	-0.64	0.52	0.38	0.83	1			
C/N	0.10	0.20	0.31	0.04	0.05	-0.03	-0.28	0.30	-0.18	0.00	0.32	0.49	-0.09	1		
DON	0.31	0.25	-0.32	0.24	0.29	0.11	-0.07	-0.19	-0.52	0.75	0.20	0.56	0.73	-0.15	1	
DOC	-0.33	-0.52	0.20	-0.44	-0.19	0.02	0.14	0.23	-0.09	-0.09	-0.03	-0.27	-0.40	0.11	-0.24	1

Abbreviations: AOA, ammonia-oxidizing archaea; AOB, ammonia-oxidizing bacteria; Clay, predicted clay content; DOC, dissolved organic carbon; DON, dissolved organic nitrogen; dw, dry weight; NS, not significant; SIAO, substrate-induced ammonia oxidation; Tot-C, total organic carbon; Tot-N, total nitrogen.

^aSpearman's correlations were used as data were not normally distributed.

Values in bold are statistically significant. *** $P \leq 0.001$; ** $P \leq 0.01$; * $P \leq 0.05$.

occasion at the site, a significant correlation was found between the AOB and of the size of the denitrifying community harboring the denitrification gene *nirK* ($r = 0.37$; $P < 0.007$ (Pearson's)). This is in agreement with the presence of *nirK* in the complete genomes of betaproteobacterial ammonia oxidizers (Jones *et al.* 2008) and the fact that the *nirK*-primers used by Enwall *et al.* (2010) amplify *nirK* also in *Nitrosospira* spp. (Garbeva *et al.*, 2007), but not in AOA (Bartossek *et al.*, 2010). The spatial patterns in the integrated farming system showed that the AOB abundance decreased when the AOA increased, indicating that AOB and AOA communities were influenced by different environmental factors. The correlations suggest that the AOB abundance was positively influenced by the soil carbon and nitrogen content, while the AOA abundance was negatively affected by increasing clay content and pH. As higher C and N content in the soil could lead to a higher mineralization rate and release of nutrients, our results imply that the AOB are favored in soils that are rich in nutrients. This is supported by recent works reporting that AOA are adapted to low-nutrient conditions (Erguder *et al.*, 2009; Martens-Habbena *et al.*, 2009). In addition, AOB have been shown to be the predominating ammonia oxidizers in nutrient-rich environments such as activated sludge (Wells *et al.*, 2009) and a sewage influenced marsh (Höfferle *et al.*, 2010). They have also been proposed to be functionally more important in nitrogen-rich environments compared with the AOA (Di *et al.*, 2009, 2010; Jia and Conrad, 2009; Zhang *et al.*, 2010). The negative correlation between AOA and clay content could be indicative of AOA being less abundant in nutrient-rich environments, as clay soils have higher cation exchange capacity and bind more ammonium. Soil pH as a differentiating factor for the AOB and AOA habitats have been discussed previously, but there are conflicting results, with some studies showing a negative correlation to pH, as in our study (Nicol *et al.*, 2008), and others showing that the AOA are negatively impacted by low pH (He *et al.*, 2007; Hallin *et al.*, 2009; Jia and Conrad, 2009; Bru *et al.*, 2010; Wessén *et al.*, 2010). Contradictory results concerning the effect of pH on AOA abundance could be explained by differences in the physiological diversity within the archaeal communities present in different soils.

The differences in the ammonia-oxidizer community structure at the different sampling locations and the different spatial distribution patterns for the AOA and AOB suggests that the environmental conditions driving the two types of ammonia-oxidizing communities were not the same. Although not obvious from the maps, the NMS ordination of the AOB communities shows a separation between the samples from the organic and integrated system. However, as the two cropping systems are not replicated and spatially separated, these differences could also be attributed to local factors at the sites.

Only weak correlations were found between the AOB or AOA community structure and the soil properties, which suggest that the major environmental factors driving the AOA and AOB community composition were not captured. However, the east-west division between the two AOB sub-communities in the integrated farming system might be explained by historical events. The division largely follows the location of a small stream that was taken away in the 1970's, but set natural estate borders in the past that potentially would affect the eastern parts of fields C3–C6. We did not observe any field-specific patterns, indicating that possible effects of recent cultivation and management practices were overridden by effects of soil properties or farming history. The observed differences in community composition among the sites were explained by differences in the relative abundance of the dominant AOB and AOA genotypes and could be assigned to specific clades in a few instances. The increase of certain AOB genotypes (TRF *Acil*-117) in the north-west areas of the integrated system related to *Nitrosospira* sp.CT2F and the eastern parts of the same system was characterized by low relative abundance of genotypes (TRF *HpyGH4IV*-417) in the clade most closely related to *Nitrosospira* sp. B6. All the retrieved AOB sequences were similar to *amoA* genes within the genus *Nitrosospira*, which is the most frequently found betaproteobacterial ammonia oxidizer in soil (Kowalchuk and Stephen, 2001). For the AOA, *AluI*-205-associated genotypes were all found in a monophyletic cluster and increased in the southern parts of the farm. These, and all but two of the retrieved AOA *amoA* sequences, were within the *Nitrososphaera gargensis* cluster that commonly dominates in soil (Prosser and Nicol, 2008).

To generate hypotheses on how microbial community structure and abundance are linked to ecosystem functions, we explored the relationship between observed patterns for the AOB and AOA communities and the related community and ecosystem functions, that is, the SIAO rates and nitrate leaching. Ecological regulation analysis, which quantifies to what extent biogeochemical fluxes are regulated by the abundance, diversity, or specific activity of the organisms performing the processes, has recently been discussed within the context of microbial ecology (Röling, 2007). Even though hierarchical regulation that is, changes in gene transcription, mRNA translation or enzyme activity at the cell level seem important with respect to changes in fluxes, the author underlined the importance of community level analyses because of the difficulty in determining the biochemical flux through every single population. Taking the individual community members into account is also hampered by the difficulty in targeting all microorganisms performing the process because of primer bias, which is also true for ammonia oxidizers (Hornek *et al.*, 2006), but which does not prevent

the application of regulation analysis (Röling, 2007). At our field site the differences in AOA, but not AOB community composition was related to the differences in nitrate leaching, indicating that some organisms might be contributing more than others to the underlying activity ultimately resulting in nitrate leaching. Logically, the nitrate leaching should relate to the ammonia-oxidation rates as the nitrite produced through ammonia oxidation is further oxidized into nitrate by the nitrite oxidizers. However, we found a negative correlation between the measured rates and the nitrate leaching, which coincided with the AOA abundance being negatively correlated with the ammonia-oxidation rates and positively related to the amount of nitrate leaching from the site. A possible explanation for this discrepancy would be that the SIAO assay favors the activity of the AOB over that of the AOA due to the high concentration of ammonia. This is supported by studies showing that the AOB prefer to grow in soils with higher ammonia substrate concentrations, while the AOA prefer to grow under low ammonia substrate concentrations (Martens-Habbena *et al.*, 2009; Di *et al.*, 2010), as discussed above. As nitrate leaching is the result of nitrification *in situ*, we speculate that nitrate leaching from the site mostly reflects the ammonia-oxidizing activity of the AOA while SIAO rates reflect the AOB activity. Only a few studies have provided direct proof for the actual contribution of AOA or AOB to ammonia oxidation (Di *et al.*, 2009; Jia and Conrad, 2009; Offre *et al.*, 2009; Zhang *et al.*, 2010), and the discrepancies between these studies have been suggested to result from differences in the amount of available ammonia (Zhang *et al.*, 2010). This further implies that the AOB and AOA are not active under the same conditions, again strengthening the idea of niche partitioning between the two groups. For a better understanding of N-cycling at the farm, we also analyzed the relationships between SIAO, nitrate leaching and potential denitrification rates using the data from Enwall *et al.* (2010). However, no significant correlation was found, which could be due to limits in existing methods for measurement of these processes (Groffman *et al.*, 2006) but also to the complexity of underlying regulatory mechanisms.

In conclusion, we have shown that bacterial and archaeal ammonia oxidizers exhibit spatial patterns at the hectare scale. The contrasting distribution patterns of AOB and AOA abundances in addition to that soil parameters were differentially correlated with the sizes of these communities indicated niche differentiation between the two groups. This is further supported by the different distributions of AOB and AOA genotypes across the sampling locations. We also showed that the two communities were related differently to community and ecosystem functions and suggest that the AOA were responsible for nitrate leaching through conversion of ammonia to nitrate via nitrite in the studied

agro-ecosystem. Findings in this study are part of a first step in identifying the 'meta-habitat' of ammonia-oxidizing communities at a scale compatible with management strategies in relation to ecosystem functioning.

Conflict of interest

The authors declare no conflict of interest.

Acknowledgements

We thank K Enwall for technical assistance. This work was supported by the Swedish Research Council for the Environment, Agricultural Sciences and Spatial Planning, Formas (contract 2009-741 and 2005-246) and the Swedish Farmers' Foundation for Agricultural Research.

References

- Altschul SF, Gish W, Miller W, Myers EW, Lipman DJ. (1990). Basic local alignment search tool. *J Mol Biol* **215**: 403–410.
- APHA (1985). *Standard Methods for the Examination of Water and Wastewater*, 16th edn. American Public Health Association: Washington, DC.
- Bartossek R, Nicol GW, Lanzen A, Klenk HP, Schleper C. (2010). Homologues of nitrite reductases in ammonia-oxidizing archaea: diversity and genomic context. *Env Microbiol* **12**: 1075–1088.
- Belser LW, Mays EL. (1980). Specific inhibition of nitrate oxidation by chlorate and its use in assessing nitrification in soils and sediments. *Appl Environ Microbiol* **39**: 505–510.
- Bru D, Ramette A, Saby NPA, Dequiedt S, Ranjard L, Jolivet C *et al.* (2010). Determinants of the distribution of nitrogen-cycling microbial communities at the landscape-scale. *ISME J*; e-pub ahead of print 12 August 2010; doi:10.1038/ismej.2010.130.
- Chen X, Zhu Y, Xia Y, Shen J, He JZ. (2008). Ammonia-oxidizing archaea: important players in paddy rhizosphere soil? *Environ Microbiol* **10**: 1978–1987.
- Conrad R. (1996). Soil microorganisms as controllers of atmospheric trace gases (H₂, CO, CH₄, OCS, N₂O, and NO). *Microbiol Rev* **60**: 609–640.
- Dequiedt S, Thioulouse J, Jolivet C, Saby NPA, Lelievre M, Maron PA *et al.* (2009). Biogeographical patterns of soil bacterial communities. *Environ Microbiol Rep* **1**: 251–255.
- Di HJ, Cameron KC, Shen JP, Winefield CS, O'Callaghan M, Bowatte S *et al.* (2009). Nitrification driven by bacteria and not archaea in nitrogen-rich grassland soils. *Nature Geosci* **2**: 621–624.
- Di HJ, Cameron KC, Shen JP, Winefield CS, O'Callaghan M, Bowatte S *et al.* (2010). Ammonia-oxidizing bacteria and archaea grow under contrasting soil nitrogen conditions. *FEMS Microbiol Ecol* **72**: 386–394.
- Enquist BJ, Kerkhoff AJ, Stark SC, Swenson NG, McCarthy MC, Price CA. (2007). A general integrative model for scaling plant growth, carbon flux, and functional trait spectra. *Nature* **449**: 218–222.
- Enwall K, Throbäck IN, Stenberg M, Söderström M, Hallin S. (2010). Soil resources influence spatial patterns of denitrifying communities at scales compatible with land management. *Appl Environ Microbiol* **76**: 2243–2250.
- Erguder TH, Boon N, Wittebolle L, Marzorati M, Verstraete W. (2009). Environmental factors shaping the ecological niches of ammonia-oxidizing archaea. *FEMS Microbiol Rev* **33**: 855–869.
- Fierer N, Carney KM, Horner-Devine MC, Megonigal JP. (2009). The biogeography of ammonia-oxidizing bacterial communities in soil. *Microb Ecol* **58**: 435–445.
- Franklin RB, Mills AL. (2003). Multi-scale variation in spatial heterogeneity for microbial community structure in an eastern Virginia agricultural field. *FEMS Microbiol Ecol* **44**: 335–346.
- Garbeva P, Baggs EM, Prosser JI. (2007). Phylogeny of nitrite reductase (*nirK*) and nitric oxide reductase (*norB*) genes from *Nitrosospira* species isolated from soil. *FEMS Microbiol Lett* **266**: 83–89.
- Green JL, Bohannan BJM, Whitaker RJ. (2008). Microbial biogeography: from taxonomy to traits. *Science* **320**: 1039–1043.
- Groffman PM, Altabet MA, Böhlke JK, Butterbach-Bahl K, David MB, Firestone MK *et al.* (2006). Methods for measuring denitrification: diverse approaches to a difficult problem. *Ecol Appl* **16**: 2091–2122.
- Grundmann GL, Debouzie D. (2000). Geostatistical analysis of the distribution of NH₄⁺ and NO₂⁻ oxidizing bacteria and serotypes at the millimeter scale along a soil transect. *FEMS Microbiol Ecol* **34**: 57–62.
- Hallin S, Jones CM, Schloter M, Philippot L. (2009). Relationship between N-cycling communities and ecosystem functioning in a 50-year-old fertilization experiment. *ISME J* **3**: 597–605.
- He JZ, Shen J, Zhang L, Zhu Y, Zheng Y, Xu M *et al.* (2007). Quantitative analyses of the abundance and composition of ammonia-oxidizing bacteria and ammonia-oxidizing archaea of a Chinese upland red soil under long-term fertilization practices. *Environ Microbiol* **9**: 2364–2374.
- Höfferle S, Nicol GW, Pal L, Hacin J, Prosser JI, Mandic-Mulec I. (2010). Ammonium supply rate influences archaeal and bacterial ammonia oxidizers in a wetland soil vertical profile. *FEMS Microbiol Ecol* **74**: 302–315.
- Hornek R, Pommerening-Röser A, Koops HP, Farnleitner AH, Kreuzinger N, Kirschner A *et al.* (2006). Primers containing universal bases reduce multiple amoA gene specific DGGE band patterns when analysing the diversity of beta-ammonia oxidizers in the environment. *J Microbiol Meth* **66**: 147–155.
- IPCC Core Writing Team, Pachauri RK, Reisinger A. (2007). *Climate Change 2007 Synthesis Report: Contribution of Working Groups I, II and III to the Fourth Assessment Report of the Intergovernmental Panel on Climate Change*. IPCC: Geneva.
- Isaaks EH, Srivastava RM. (1989). *An introduction to Applied Geostatistics*. Oxford University Press: New York.
- Jia ZJ, Conrad R. (2009). Bacteria rather than Archaea dominate microbial ammonia oxidation in an agricultural soil. *Environ Microbiol* **11**: 1658–1671.
- Jones CM, Stres B, Rosenquist M, Hallin S. (2008). Evolutionary history of denitrification as assessed by phylogenetic analysis of nitrite, nitric oxide and nitrous oxide respiratory enzymes. *Molec Biol Evol* **25**: 1955–1966.

- Könneke M, Bernhard AE, de la Torre JR, Walker CB, Waterbury JB, Stahl DA. (2005). Isolation of an autotrophic ammonia-oxidizing marine archaeon. *Nature* **437**: 543–546.
- Kowalchuk GA, Stephen JR. (2001). Ammonia-oxidizing bacteria: a model for molecular microbial ecology. *Annu Rev Microbiol* **55**: 485–529.
- Leininger S, Urich T, Schloter M, Schwark L, Qi J, Nicol GW *et al.* (2006). Archaea predominate among ammonia-oxidizing prokaryotes in soils. *Nature* **442**: 806–809.
- Mantel N. (1967). Detection of disease clustering and a generalized regression approach. *Cancer Res* **27**: 209–220.
- Martens-Habbena W, Berube PM, Urakawa H, de la Torre JR, Stahl DA. (2009). Ammonia oxidation kinetics determine niche separation of nitrifying Archaea and Bacteria. *Nature* **461**: 976–979.
- Mertens J, Broos K, Wakelin SA, Kowalchuk GA, Springael D, Smolders E. (2009). Bacteria, not archaea, restore nitrification in a zinc-contaminated soil. *ISME J* **3**: 916–923.
- Moran PAP. (1950). Notes on continuous stochastic phenomena. *Biometrika* **37**: 17–23.
- Nicol GW, Leininger S, Schleper C, Prosser JI. (2008). The influence of soil pH on the diversity, abundance and transcriptional activity of ammonia oxidizing archaea and bacteria. *Environ Microbiol* **10**: 2966–2978.
- Offre P, Prosser JI, Nicol GW. (2009). Growth of ammonia-oxidizing archaea in soil microcosms is inhibited by acetylene. *FEMS Microbiol Ecol* **70**: 99–108.
- Pearson K. (1896). Mathematical contributions to the theory of evolution. III. Regression, heredity and panmixia. *Phil Trans R Soc, Ser A* **187**: 253–318.
- Philippot L, Bru D, Saby NPA, Cuhel J, Arrouays D, Simek M *et al.* (2009a). Spatial patterns of bacterial taxa in nature reflect ecological traits of deep branches of the 16S rRNA bacterial tree. *Environ Microbiol* **11**: 3096–3104.
- Philippot L, Cuhel J, Saby NPA, Cheneby D, Chronakova A, Bru D *et al.* (2009b). Mapping field-scale spatial patterns of size and activity of the denitrifier community. *Environ Microbiol* **11**: 1518–1526.
- Prosser JI, Nicol GW. (2008). Relative contributions of archaea and bacteria to aerobic ammonia oxidation in the environment. *Environ Microbiol* **10**: 2931–2941.
- Ritz K, McNicol W, Nunan N, Grayston S, Millard P, Atkinson D *et al.* (2004). Spatial structure in soil chemical and microbiological properties in an upland grassland. *FEMS Microbiol Ecol* **49**: 191–205.
- Röling WFM. (2007). Do microbial numbers count? Quantifying the regulation of biogeochemical fluxes by population size and cellular activity. *FEMS Microbiol Ecol* **62**: 202–210.
- Rothauwe JH, Witzel KP, Liesack W. (1997). The ammonia monooxygenase structural gene *amoA* as a functional marker: Molecular fine-scale analysis of natural ammonia-oxidizing populations. *Appl Environ Microbiol* **63**: 4704–4712.
- Sahan E, Muyzer G. (2008). Diversity and spatio-temporal distribution of ammonia-oxidizing Archaea and Bacteria in sediments of the Westerschelde estuary. *FEMS Microbiol Ecol* **64**: 175–186.
- Savage VM, Webb CT, Norberg J. (2007). A general multi-trait-based framework for studying the effects of biodiversity on ecosystem functioning. *J Theor Biol* **247**: 213–229.
- Schauss K, Focks A, Leininger S, Kotzerke A, Heuer H, Thiele-Bruhn S *et al.* (2009). Dynamics and functional relevance of ammonia-oxidizing archaea in two agricultural soils. *Environ Microbiol* **11**: 446–456.
- Shen JP, Zhang LM, Zhu YG, Zhang JB, He JZ. (2008). Abundance and composition of ammonia-oxidizing bacteria and ammonia-oxidizing archaea communities of an alkaline sandy loam. *Environ Microbiol* **10**: 1601–1611.
- Spearman C. (1904). The proof and measurement of association between two things. *Am J Psychol* **15**: 72–101.
- Stamatakis A. (2006). RAxML-VI-HPC: maximum likelihood-based phylogenetic analyses with thousands of taxa and mixed models. *Bioinformatics* **22**: 2688–2690.
- Stamatakis A, Hoover P, Rougemont J. (2008). A fast bootstrapping algorithm for the RAxML web-servers. *Syst Biol* **57**: 758–771.
- Stenberg B, Johansson M, Pell M, Sjö Dahl-Svensson K, Stenström J, Torstensson L. (1998). Microbial biomass and activities in soil as affected by frozen and cold storage. *Soil Biol Biochem* **30**: 393–402.
- Thompson JD, Higgins DG, Gibson TJ. (1994). CLUSTAL W: improving the sensitivity of progressive multiple sequence alignment through sequence weighting, position-specific gap penalties and weight matrix choice. *Nucleic Acids Res* **22**: 4673–4680.
- Torstensson L. (1993). Guidelines. Soil Biological Variables In Environmental Hazard Assessment. Report No. 4262. Swedish Environmental Protection Agency: Solna.
- Tourna M, Freitag TE, Nicol GW, Prosser JI. (2008). Growth, activity and temperature responses of ammonia-oxidizing archaea and bacteria in soil microcosms. *Environ Microbiol* **10**: 1357–1364.
- Treusch AH, Leininger S, Kletzin A, Schuster SC, Klenk HP, Schleper C. (2005). Novel genes for nitrite reductase and Amo-related proteins indicate a role of uncultivated mesophilic crenarchaeota in nitrogen cycling. *Environ Microbiol* **7**: 1985–1995.
- Venter JC, Remington K, Heidelberg JF, Halpern AL, Rusch D, Eisen JA *et al.* (2004). Environmental genome shotgun sequencing of the Sargasso Sea. *Science* **304**: 66–74.
- Wells GF, Park HD, Yeung CH, Eggleston B, Francis CA, Criddle CS. (2009). Ammonia-oxidizing communities in a highly aerated full-scale activated sludge bioreactor: betaproteobacterial dynamics and low relative abundance of Crenarchaea. *Environ Microbiol* **11**: 2310–2328.
- Wessén E, Nyberg K, Jansson JK, Hallin S. (2010). Responses of bacterial and archaeal ammonia oxidizers to soil organic and fertilizer amendments under long-term management. *Appl Soil Ecol* **45**: 193–200.
- Wetterlind J, Stenberg B, Söderström M, Stenberg M. (2005). New strategy for farm-soil mapping using near infrared spectroscopy to increase sample point density. In: Burling-Claridge GR *et al.* (eds). *Proceedings of NIR in Action—Making a difference*. IM Publications: Chichester, pp 299–303.
- Zhang LM, Offre PR, He JZ, Verhamme DT, Nicol GW, Prosser JI. (2010). Autotrophic ammonia oxidation by soil thaumarchaea. *Proc Natl Acad Sci USA* **107**: 17240–17245.
- Zhou J, Kang S, Schadt CW, Garten CT. (2008). Spatial scaling of functional gene diversity across various microbial taxa. *Proc Natl Acad Sci USA* **105**: 7768–7773.

Supplementary Information accompanies the paper on The ISME Journal website (<http://www.nature.com/ismej>)